Title
Convective distribution of tropospheric ozone and tracers in the Central American ITCZ region: Evidence from observations during TC4

Journal
Journal of Geophysical Research, 115(D10)

ISSN
0148-0227

Authors
Avery, Melody
Twohy, Cynthia
McCabe, David
et al.

Publication Date
2010

DOI
10.1029/2009jd013450

Convective distribution of tropospheric ozone and tracers in the Central American ITCZ region: Evidence from observations during TC4

Melody Avery,[1] Cynthia Twohy,[2] David McCabe,[3] Joanna Joiner,[4] Kurt Severance,[5] Eliot Atlas,[6] Donald Blake,[7] T. P. Bui,[8] John Crounse,[3] Jack Dibb,[9] Glenn Diskin,[10] Paul Lawson,[11] Matthew McGill,[12] David Rogers,[2] Glen Sachse,[13] Eric Scheuer,[9] Anne M. Thompson,[14] Charles Trepte,[1] Paul Wennberg,[3] and Jerald Ziemke[15]

Received 28 October 2009; revised 17 May 2010; accepted 7 June 2010; published 13 October 2010.

[1] During the Tropical Composition, Clouds and Climate Coupling (TC4) experiment that occurred in July and August of 2007, extensive sampling of active convection in the ITCZ region near Central America was performed from multiple aircraft and satellite sensors. As part of a sampling strategy designed to study cloud processes, the NASA ER-2, WB-57 and DC-8 flew in stacked "racetrack patterns" in convective cells. On July 24, 2007, the ER-2 and DC-8 probed an actively developing storm and the DC-8 was hit by lightning. Case studies of this flight, and of convective outflow on August 5, 2007 reveal a significant anti-correlation between ozone and condensed cloud water content. With little variability in the boundary layer and a vertical gradient, low ozone in the upper troposphere indicates convective transport. Because of the large spatial and temporal variability in surface CO and other pollutants in this region, low ozone is a better convective indicator. Lower tropospheric tracers methyl hydrogen peroxide, total organic bromine and calcium substantiate the ozone results. OMI measurements of mean upper tropospheric ozone near convection show lower ozone in convective outflow. A mass balance estimation of the amount of convective turnover below the tropical tropopause transition layer (TTL) is 50%, with an altitude of maximum convective outflow located between 10 and 11 km, 4 km below the cirrus anvil tops. It appears that convective lofting in this region of the ITCZ is either a two-stage or a rapid mixing process, because undiluted boundary layer air is never sampled in the convective outflow.

Citation: Avery, M., et al. (2010), Convective distribution of tropospheric ozone and tracers in the Central American ITCZ region: Evidence from observations during TC4, *J. Geophys. Res.*, *115*, D00J21, doi:10.1029/2009JD013450.

1. Introduction

1.1. TC4 Mission and Goals of This Paper

[2] This paper describes observations of trace gas redistribution by convection in the tropical troposphere, in the vicinity of the inter-tropical convergence zone (ITCZ) in the Gulf of Panama near Central America. Observational process studies to characterize vertical tracer transport and associated chemistry in strong tropical convection are needed to understand carbon and nitrogen budgets, and the oxidizing capacity of the atmosphere. Although convection is

[1]Atmospheric Composition Branch, Science Directorate, NASA Langley Research Center, Hampton, Virginia, USA.
[2]Department of Oceanic and Atmospheric Science, Oregon State University, Corvallis, Oregon, USA.
[3]Chemistry Department, California Institute of Technology, Pasadena, California, USA.
[4]Atmospheric Chemistry and Dynamics Branch, NASA Goddard Space Flight Center, Greenbelt, Maryland, USA.
[5]Systems Engineering Directorate, NASA Langley Research Center, Hampton, Virginia, USA.
[6]Division of Marine and Atmospheric Chemistry, Rosenstiel School of Marine and Atmospheric Sciences, University of Miami, Miami, Florida, USA.

0148-0227/10/2009JD013450

[7]School of Physical Sciences, University of California, Irvine, California, USA.
[8]Atmospheric Science Branch, Earth Science Division, NASA Ames Research Center, Moffett Field, California, USA.
[9]Institute for the Study of Earth, Oceans, and Space, University of New Hampshire, Durham, New Hampshire, USA.
[10]Chemistry and Dynamics Branch, NASA Langley Research Center, Hampton, Virginia, USA.
[11]SPEC Inc., Boulder, Colorado, USA.
[12]Mesoscale Atmospheric Processes Branch, NASA Goddard Space Flight Center, Greenbelt, Maryland, USA.
[13]National Institute of Aerospace, Hampton, Virginia, USA.
[14]Department of Meteorology, Pennsylvania State University, University Park, Pennsylvania, USA.
[15]Goddard Earth Sciences and Technology Center, University of Maryland Baltimore County, Baltimore, Maryland, USA.

the dominant process controlling tropical tracer distribution, chemical transport models have difficulty simulating convective transport and chemistry accurately due to the dominance of small-scale diabatic processes. It is important to accurately quantify transport and chemistry of chemical tracers in the tropics because there is an abundance of energy available for phase transformation and photochemistry, and there is strong coupling between chemistry, clouds and climate impacts. Finally, the planetary boundary layer has the most potential for direct impact on the stratosphere in the tropics.

[3] The measurements described here were taken from the NASA DC-8, WB-57, ER-2, balloon sondes and the NASA Aura satellite during the Tropical Composition, Cloud and Climate Coupling Experiment (TC4), July 17 – August 8 of 2007. TC4 science goals, flight planning and flight summaries are described in the TC4 overview paper by *Toon et al.* [2010]. The TC4 mission included sampling from the DC-8 as a moderate altitude platform, from the WB-57 for higher altitude sampling in the tropical transition layer (TTL, from 12 to 17 km) just below the stratosphere, and highest altitude sampling from the ER-2 with remote sensors similar to many found on NASA Earth Observing System (EOS) satellites. Whenever feasible, aircraft flights were planned to be coincident with an EOS satellite overpass, in order to validate the satellite instrument observations, or to combine them with the suborbital in situ and remote measurements for analysis.

[4] The scope of the TC4 mission included measurements to quantify cloud composition and physics, tropospheric and lower stratospheric composition and chemistry, and vertical transport by convection. In this paper we focus on addressing a few of the major TC4 science questions by analyzing data in the troposphere. These science questions are paraphrased here: "What is the composition of the tropical troposphere below the TTL"? "What are the mechanisms that control ozone within and below the TTL"? "What is the chemical nature of the convective outflow"?

1.2. Origin of Ozone in the Upper Troposphere

[5] Ozone is important for determining the oxidizing capacity of the atmosphere, and it is both an infrared and visible wavelength absorber, which either heats or cools the atmosphere locally, depending on altitude. Processes that control ozone in the tropical upper troposphere (500–150 hPa) are expected to be predominantly convective outflow from the boundary layer, extra-tropical advection, and in situ photochemical production. The chemical lifetime for ozone loss is about 50 days in the tropical upper troposphere [*Folkins et al.*, 2006b], compared to the typical vertical mixing time of less than 1 day during TC4 [*Pfister et al.*, 2010], so that ozone can be used as a dynamical tracer for vertical transport if in situ ozone production is not too large.

[6] In situ ozone production can be enhanced by biomass burning plumes containing NO_X, or downwind of electrically active convection by NO produced by lightning [*Pickering et al.*, 1996]. Direct production of ozone by lightning is difficult to measure, and apparently rare [*Ridley et al.*, 2006]. No ozone production was observed during a lightning strike to the DC-8 during TC4. In the tropics there is generally plenty of water vapor and sunlight available to form reactive odd hydrogen-containing radicals ($OH^+HO_2 \equiv HO_x$), and carbon monoxide or hydrocarbons from biomass burning are often available for oxidation and ozone production. However, ozone is also destroyed very effectively and catalytically by HOx if HO_2 is not efficiently converted to OH by the oxidation and cycling of NO and NO_2 radicals (NO_x). In general, ozone formation is NO_x -limited in the tropical TC4 study region.

[7] Tracer sampling of the upper troposphere during TC4 mainly showed well-aged pollution, well mixed into a clean tropical background. Estimates of the ozone production rate range between 0.2 parts per billion by volume (ppbv)/hour expected from calculations published by *Folkins et al.* [1999] in the clean tropical upper troposphere to 0.8 ppbv/hour from the tropical biomass burning case studied by *Pickering et al.* [1996]. Ozone production rates of up to 0.5 ppbv/hour were calculated during TC4 by R. Salawitch (personal communication, 2009, plot not shown). G. A. Morris et al. (Observations of ozone production in a dissipating convective cell during TC4, submitted to *Journal of Geophysical Research*, 2010) measured even higher ozone production rates of 1.1–3.2 ppb/hour between 2 and 5 km in a convective cloud. This suggests that in situ ozone production can sometimes occur vigorously during vertical transport in convection.

1.3. Meteorology During TC4 and Vertical Transport

[8] The TC4 study area was chosen to be in the vicinity of the ITCZ so that the aircraft, balloons and satellite sensors could sample active convection [*Toon et al.*, 2010]. During July and August of 2007, Special Sensor Microwave Imager (SSM/I) rainfall images show that maximum rainfall from the ITCZ was located in the Gulf of Panama, in the center of the TC4 study area. Sea surface temperature anomalies in the Eastern Pacific were 1–1.5 degrees below average, indicating the onset of a moderate cold-phase ENSO event (NOAA Climate Prediction Center, Diagnostic Discussion). Comparison with other years showed less convection and less intense convection during 2007 than usual [*Pfister et al.*, 2010], with stronger than usual easterlies in the upper troposphere that are typical of the cold phase of ENSO. Examination of the wind measurements during local sampling in the upper troposphere from the DC-8 using the Meteorological Measurement System (MMS) [*Scott et al.*, 1990] confirms that > 90% of the wind vectors have an easterly component.

[9] Winds measured in the mid-troposphere during local flights on the DC-8 also almost always show an easterly component, with a slight bias to the south compared to the upper tropospheric winds. However, winds at the surface in the planetary boundary layer are much more complex. Large-scale data analysis [*Pfister et al.*, 2010] and dust collected from low altitude sampling shows that the lower level winds brought air from Africa and South America into the boundary layer in the main TC4 study region, while vector winds measured on the DC-8 show winds coming from all 4 quadrants, and chemical tracers showed a mix of both polluted continentally influenced air and very clean maritime air, as discussed below. While convection in the ITCZ region in 2007 was relatively weak, analysis by D. Hlavka et al. (Vertical cloud climatology during TC4 derived from high-altitude aircraft merged lidar and radar, submitted to *Journal of Geophysical Research*, 2010) shows that the TC4 local

study area was still very cloudy, with on average greater than 94% multilayered cloud cover, most frequently marine stratus decks overlain with cirrus from evolving convective anvils. Further, periods of active convection were sampled by the airplanes, particularly at the beginning and at the end of the mission.

1.4. Summary

[10] In this paper we look at the impact of these dynamics on the composition of the upper troposphere in the TC4 study region. First we present an overview of the distribution and correlations of O_3, CO and CH_4, and focus on the composition of the boundary layer source region. Two case studies are presented during which the planes sampled active convection and convective outflow. These provide an opportunity to establish whether there are potentially robust tracer correlations in the extensive DC-8 data set in convectively influenced air. During these two flights, the inverse relationship between condensed cloud water content (both water and ice) and ozone is the strongest we found in the fast-response in situ data set, so we test the larger ensemble of upper tropospheric data from the "racetrack" flights to see if this relationship appears to be true more universally. Since it does, we use this information to find the altitude of maximum convective outflow, and compare our results with ozonesonde data and with vertical boundary layer tracer distribution.

2. Observations and Methods of Analysis

2.1. In Situ Aircraft Data

[11] The in situ data that we use in this paper were taken from the NASA DC-8 and WB-57 by various investigators as described here. The list of chemical and physical data considered and analyzed in this paper includes ozone, carbon monoxide, methane, condensed cloud water content, organic bromine, peroxy nitric acid, calcium and methyl hydrogen peroxide. Other reactive nitrogen species are discussed more generally, but are not used for analysis because in this active convective region most reactive nitrogen species are not conserved, and these tracer relationships are chaotic.

[12] The ozone, carbon monoxide, methane and condensed cloud water content data on the DC-8 are available at one-second-time resolution, corresponding to a horizontal resolution of about 200 m. The location of sampling for each of these constituents on the DC-8 is shown in Figure 5 of *Toon et al.* [2010]. Merged data files have been created, with all data aligned to the time stamp of water vapor data measured by the Langley DLH diode laser hygrometer, an open-path measurement without sample lag considerations. Ozone was measured using fast-response nitric oxide chemiluminesence [*Fairlie et al.*, 2007; *Pearson and Stedman*, 1980]. Carbon monoxide and methane were measured using a tunable diode laser-based absorption technique by the Differential Absorption for CO Measurements (DACOM) instrument [*Sachse et al.*, 1987].

[13] Measurements of the condensed cloud water content (CWC) were made by the NCAR counterflow virtual impactor (CVI) described by *Twohy et al.* [1997].

[14] During the ER-2 and DC-8 flights that occurred on July 24, 2007, the DC-8 flew through developing convective cores with large vertical velocities and corresponding CWC. The CVI instrument, while normally accurate to within 15% [*Twohy et al.*, 1997], relies on subisokinetic enhancement of condensed water to measure low concentrations, and requires manual adjustment to measure high water contents such as are present in convective cells. Since these were not anticipated for the July 24th flight, the CVI signal was saturated twice during the flight when the DC-8 passed through convective turrets. CWC content derived from the SPEC 2DS cloud probe data [*Lawson et al.*, 2006, 2010] are also used during this flight in vigorous convection, since the probe did not saturate. The 2DS integrates the cloud particle size distribution to obtain condensed water and this technique generally agreed well with the CVI measurement during the rest of the TC-4 mission.

[15] The Meteorological Measurement System (MMS) provided accurate, high resolution pressure, temperature and wind data used in this analysis for both the DC-8 and the WB-57, using instrumentation similar to that described for the ER-2 by *Scott et al.* [1990]. Ozone data from the WB-57 were measured using a dual beam ultraviolet photometer. We also compare the aircraft data with ozone data measured from sondes using electrochemical cells from *Thompson et al.* [2010] and Morris et al. (submitted manuscript, 2010).

[16] We compared the vertical distribution of some other trace gases to our results from examining ozone. Methyl hydrogen peroxide (MHP) and PNA (peroxy-nitric acid) were measured using a chemical ion mass spectrometer (CIMS) technique developed at the California Institute of Technology [*Spencer et al.*, 2009]. Total organic bromine was calculated from individual species measured by analysis of whole air samples using gas chromatography at the University of Miami for the WB-57 and the University of California, Irvine for the DC-8. Calcium was analyzed from bulk aerosol composition measurements made from the NASA DC8 by the University of New Hampshire soluble acidic gases and aerosols (SAGA) instrument [*Dibb et al.*, 2003].

2.2. Suborbital and Satellite-Based Remotely Sensed Data

[17] Cloud images from the Cloud Physics Lidar (CPL) on the ER-2 were used to locate aircraft measurements from the DC-8 relative to the cloud top height and cloud morphology. The CPL cloud images are a time series of 532 nm attenuated backscatter profiles, measured as described by *McGill et al.* [2002]. During TC4 there were several near coincidences between overpasses by the CALIPSO satellite and the multiple-aircraft flight tracks, and we show a comparison between cloud images from the CALIOP instrument [*Winker et al.*, 2007], the CPL on the ER-2 and in situ CVI measurements of CWC as a movie (see section 2.3, below).

[18] We evaluate mean tropospheric ozone volume mixing ratios calculated between the tropopause and sampling by the DC-8 that are derived using the NASA Aura Ozone Monitoring Instrument (OMI) [*Levelt et al.*, 2006], and the Microwave Limb Sounder (MLS). The tropospheric ozone column residual is first determined by subtracting interpolated MLS version 2.2 stratospheric column ozone [*Froidevaux et al.*, 2008] from the OMI-TOMS [*McPeters et al.*, 2008] measured column ozone for each OMI pixel. This measured column does not include ozone that is shielded from the satellite by clouds.

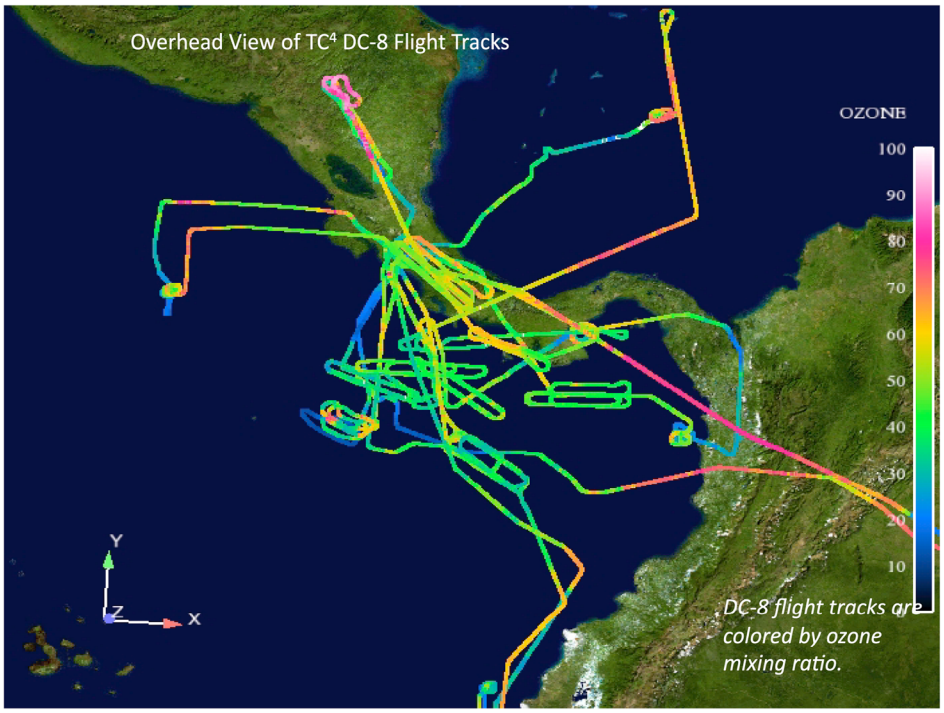

Figure 1. TC4 local "racetrack" flights: Flight tracks of the NASA DC-8 are shown from above, colored by the amount of in situ ozone measured along the way. The flight tracks shown here represent the location of data collected and used in this paper for analysis of the convective outflow region in the upper troposphere. During these flights the DC-8 flight planning featured extensive sampling of active convection or convective outflow in close proximity to the aircraft home base in Alajuela, Costa Rica. Many of the flights show a characteristic "racetrack" pattern, maintained while 2 or 3 planes were stacked vertically.

[19] Ozone mean volume mixing ratio is then calculated by dividing this partial column by the difference between the tropopause pressure and the effective scene pressure (P_{eff}, in hPa) [e.g., *Ziemke et al.*, 2001; *Joiner et al.*, 2009]. P_{eff} is given by:

$$P_{eff} = (1 - f)P_s + fP_c \quad (1)$$

In equation 1, P_s is the surface pressure, P_c is the optical centroid cloud pressure, and f is the fraction of total radiance coming from the cloudy portion of a pixel. The optical centroid cloud pressure is derived from the OMI rotational-Raman cloud algorithm [*Joiner and Vasilkov*, 2006] and appropriately accounts for the shielding effect of clouds in the OMI-TOMS ultraviolet retrieval algorithm [*Vasilkov et al.*, 2008]. The initial derivation of tropospheric ozone from the OMI-MLS residual technique by *Schoeberl et al.* [2007] did not fully account for cloud effects. The derived column-averaged mixing ratio derived here is representative of the tropospheric column above the P_{eff}. When we extrapolate that mixing ratio to the surface, the global correlation between the OMI/MLS-derived 200 hPa to surface column ozone and that from ozonesondes improved from about 0.6 to 0.8 [*Joiner et al.*, 2009]. To our knowledge, this is the best agreement ever obtained between the ozonesonde measurements (point measurements that contain a significant amount of variability in both space and time) and satellite data that represent an average over a much larger area. This demonstrates that tropospheric ozone can be accurately derived using the residual technique in both clear and cloudy conditions.

2.3. Data Synthesis and Analysis Strategy

[20] In situ data from the DC-8 were merged as described above, with 1-s time resolution and a corresponding approximate horizontal resolution of 200 m. The DC-8 data set in the upper troposphere extends between 8.5 and 12.2 km, with a corresponding potential temperature range of 330–350 K. We created a DC-8 data ensemble from sampling during the local "racetrack" flights with a limited geographical domain between 4 and 10 N latitude, and between 79–87 W longitude. The flights used occurred on July 17, 22, 24 and 31, and August 3, 5, and 8 of 2007, and these are shown in Figure 1, with the DC-8 flight track colored by in situ ozone amount. The ER-2 flew as well on these days, with the degree of flight coordination increasing with practice as the mission progressed. Flight coordination is discussed extensively by *Toon et al.* [2010]. The WB-57 also flew a coordinated pattern during the three August flights.

[21] Merging and interpreting the remote and in situ data together is challenging. We developed a special-purpose program to combine the CPL and CALIOP images and DC-8 data, as well as their geo-location and time stamp information, into geometry and scalar-data files compatible with the COTS 3-D Visualization software tool called "EnSight." These data sets could then be co-located in space and time, with respect to a map of the Earth built

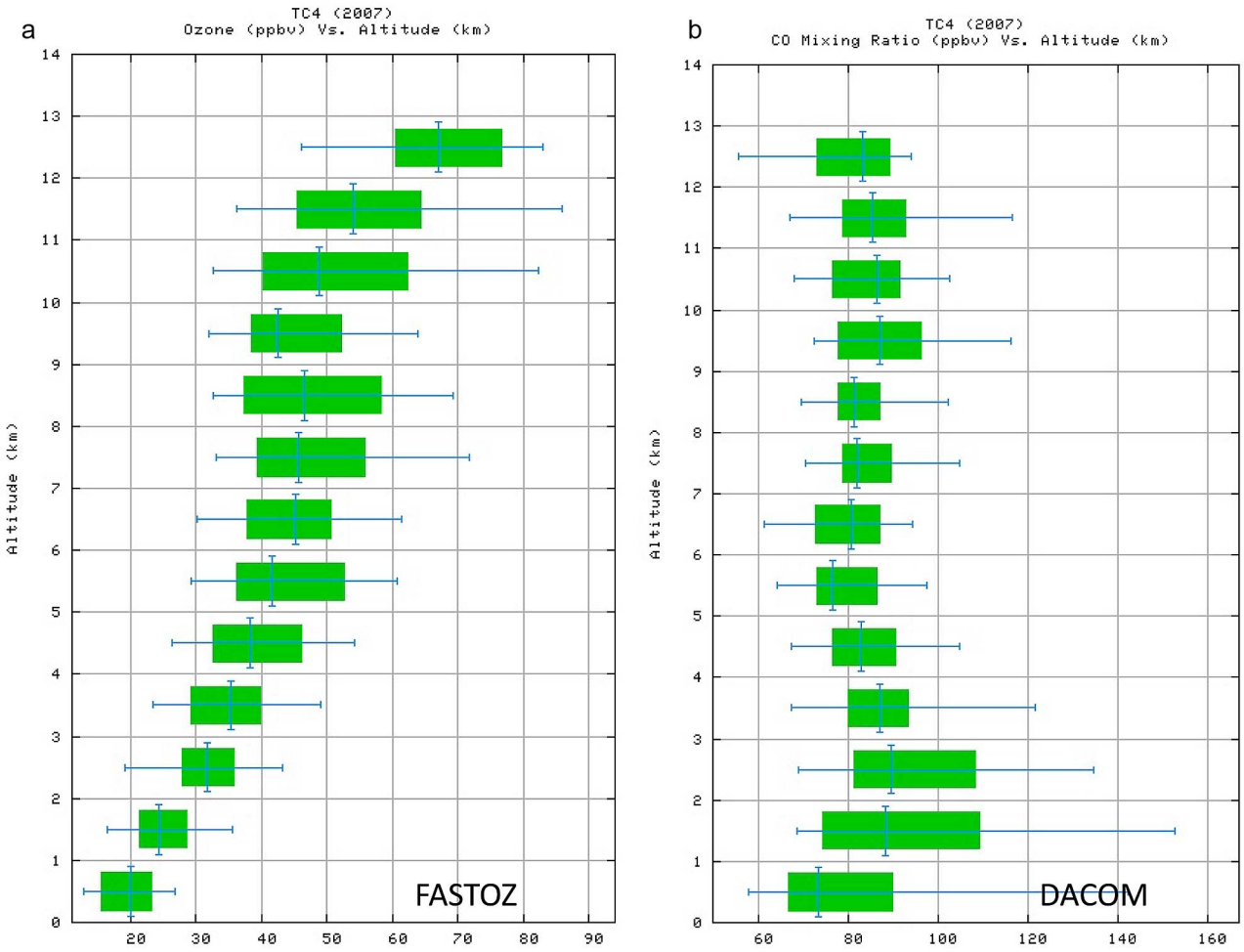

Figure 2. TC4 (a) ozone and (b) carbon monoxide median profiles, 75N–17N, 270W–290W: profiles of the median, the first and third quartile (green boxes), and the 5–95% distribution (whiskers) of the in situ ozone and carbon monoxide measured from the NASA DC-8 by FASTOZ and DACOM during TC4. Data taken between 7S and 17N latitude, and between 70 and 90W longitudes, is averaged to 30 s and binned in 1 km intervals for all the TC4 flights.

from the GTOPO30 digital elevation model (DEM) and the NASA Blue Marble cloud-free image. The visualization software provided both 3-D movies and stills of the combined data set, providing a powerful and intuitive way to spatially and temporally link the observations, and to build intuition for data analysis decisions. A movie showing the precise correspondence between a CALIOP cloud image from the August 5th CALIPSO overpass, the corresponding CPL cloud image from the ER-2, and in situ cloud water content from the DC-8 is available as auxiliary material Movie S1.[1]

3. Results and Discussion

3.1. Overview of in Situ Observed Tropospheric Composition

[22] To provide an overview of the larger context of the background tropical tropospheric chemical composition of the tropical tropospheric study area, we have plotted the aggregate median vertical profile and statistical distribution of ozone and carbon monoxide, shown as Figure 2. We look at ozone and carbon monoxide because neither gas is soluble in the cloudy tropical environment, and they both have similar chemical lifetimes of about 50–60 days, much longer than the vertical mixing time of less than 1 day. The tracer data are binned at 1 km resolution, and includes all of the measurements from the DC-8 between 7S and 17 N latitude, and between 70–90 W longitude.

[23] The median ozone profile shows a characteristic tropical "S"-shape [*Folkins et al.*, 2002], with depleted ozone in the boundary layer, some ozone enhancement in the middle troposphere, a minimum caused by convective outflow in the upper troposphere, between 9 and 10 km, and a monotonically increasing ozone gradient above the outflow maximum. In the upper troposphere, enhanced ozone of more than 65 ppbv occurs in less than 25% of the data, except above 12 km, with potential temperatures approaching or greater than 350K. Based on this, in this paper when we refer to "high" ozone, we mean specifically ozone concentrations greater than 65 ppbv. Ozone in the boundary layer is both

[1] Auxiliary materials are available in the HTML. doi:10.1029/2009JD013450.

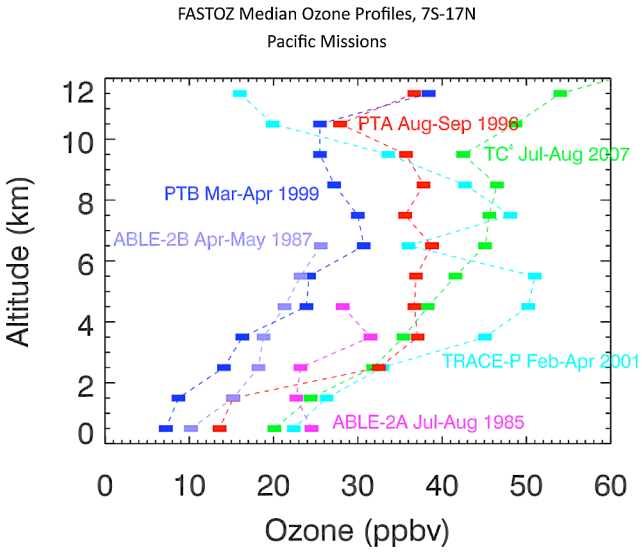

Figure 3. Profiles of the median ozone concentration calculated using 30 s averaged data sampled between 7S and 17N latitude during various aircraft field missions over the tropical Pacific and Western Atlantic oceans. The data are binned at 1 km vertical resolution, and extends over the same latitudinal range of the tropics as does the TC4 mission. The historical data are shown as context for comparison with the TC4 data, which are shown in green. Data from each mission are annotated with a color-coded label listing the mission timeframe.

low and strikingly uniform throughout the sample region. Correlation during boundary layer sampling with MMS wind measurements shows that ozone measured while winds have an easterly component (60–110 degrees) has the smallest range (19–25 ppbv), while ozone measured while winds have a southerly or westerly component has a slightly wider range (12–28 ppbv). A probability distribution of boundary layer ozone shows the median value to be about 21 ppbv, with less than 10 ppbv of variability everywhere, and no significant difference (0.5 ppbv) between the Atlantic and the Pacific marine boundary layers. This suggests that catalytic destruction of ozone by reactive hydrogen radicals (HOx) removes ozone efficiently in the lowermost atmosphere. This appears to be the case in both the marine boundary layer, and in measurements over land. Comparison with the more polluted NATIVE surface ozone data set from Las Tables, Panama [*Thompson et al.*, 2010, Figure 10] also shows surface ozone averages near 20 ppbv.

[24] The carbon monoxide median profile is very uniform vertically, with medians between 70 and 90 ppbv throughout the troposphere. This contrasts with the large range of CO measured in the boundary layer, between 55 and 155 ppbv with the 75th percentile occurring at 90 ppbv. An examination of DACOM measurements of CO at take-off and landing at Alajuela airport shows a large amount of day-to-day variability, despite its proximity to San Jose. Comparison of the aircraft CO measurements by DACOM with surface measurements of CO from the NATIVE trailer in Panama show that the Panama site was relatively polluted, since 75% of the boundary layer aircraft measurements show CO of 90 ppbv or less, while all of the NATIVE data indicate CO of 90 ppbv or more [*Thompson et al.*, 2010].

[25] Carbon monoxide is usually the product of incomplete combustion, but the convectively active TC4 region does not show much fresh pollution or biomass-burning enhancement. This is substantiated by measurements of HCN, a biomass-burning tracer that is also not enhanced above a moderate background level in the convective area. The relationship between ozone and carbon monoxide is complex, and varies by flight day. Positive correlations can indicate aged pollution or very clean air; negative correlations can indicate stratospheric influence, in situ ozone production from lightning NO_x, biogenic influence, or fresh smoke. Because of these ambiguities, it is difficult to use the correlations to provide much useful information about air mass history. In the TC4 study region, CO is not a useful tracer for convective transport because of convective lofting of both clean and dirty lower tropospheric air. During the convective "racetrack" flights, either a positive or a negative correlation between CO and O_3 tends to persist for all altitudes sampled, reflecting the influence of either a clean or a polluted boundary layer on an individual day. A composite CO:O_3 correlation plot for the mission shows no significant correlation, or any distinct plumes, indicating that a very large amount of mixing has occurred in this region. Our results suggest that care must be used in interpreting CO:O_3 relationships in convection over combined marine and terrestrial environments.

[26] For context, in Figure 3 we look at the vertical ozone distribution during TC4 compared with ozone measured at similar latitudes during other aircraft field missions. The comparison is facilitated because these measurements were all made using NASA Langley NO chemiluminesence detectors, with an estimated 3% accuracy [*Avery et al.*, 2001; *Fairlie et al.*, 2007; *Pearson and Stedman*, 1980]. Further, all but the ABLE-2B mission occurred during a mild ENSO cold phase. Figure 3 shows the median ozone concentration measured in 1 km bins as a function of altitude. We show the ABLE-2A (Jul–Aug, 1985) and 2B (Apr–May, 1987) missions, with sampling over the Amazon basin and Western Atlantic, the PEM Tropics A and B (PTA Aug–Sep, 1996 and PTB Mar–Apr, 1999) missions with pan-Pacific tropical sampling, and the TRACE-P (Feb–Apr 2001) mission, which featured Asian air pollution and sampling of the Western Pacific.

[27] The largest difference in tropospheric ozone appears to be seasonal, with roughly double the amount of ozone occurring in the boundary layer during July–October than during February–May. This seasonal difference persists in the middle and upper troposphere, where there was about 10 ppbv more ozone measured during TC4 in July–August than there was during PTA in August–September, most likely due to the difference between sampling the remote Pacific and the TC4 study area around Central America. The TRACE-P mission was unusual in targeting Asian pollution, with a resulting high mid-tropospheric ozone median. Unfortunately, the ABLE-2A measurements do not extend higher than 5 km, but these show that ozone was a bit lower in the lower troposphere over the Amazon basin than measured during TC4. This may be because the tropical rain forest is a very efficient sink for ozone. This was discussed in detail by *Gregory et al.* [1988], describing the ABLE-2A measurements. Our TC4 measurements from a boundary

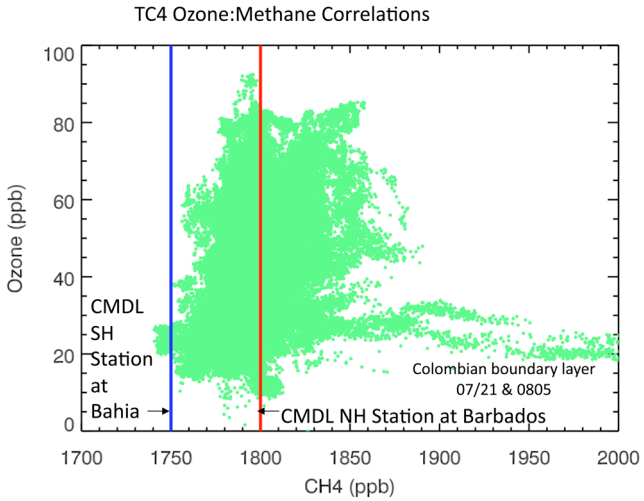

Figure 4. A plot of ozone concentrations versus methane measured using the DACOM instrument. They are uncorrelated, and this reflects how well mixed the air is in the TC4 study area of active tropical convection. NOAA CMDL measurements of methane from the closest Southern and Northern Hemispheric surface sampling stations are shown for comparison with the aircraft measurements. There is no stratospheric air, which would appear in the upper left corner of this plot.

layer leg over the Peruvian rain forest substantiate this. This boundary layer leg had the lowest average ozone concentration measured during TC4 (11 ppbv) and the highest CO (153 ppbv), produced from oxidized hydrocarbons.

[28] Methane and ozone from TC4 are shown in Figure 4. These are mainly uncorrelated, with the exception of two plumes containing very high biogenic methane sampled in the Colombian boundary layer, once over land, and once just off the Pacific coast. The distribution looks very similar to ozone correlations with CO, and this plot is shown to illustrate the well-mixed state of the free troposphere during TC4. Methane concentrations measured at the NOAA CMDL ground stations in the Northern and Southern Hemisphere (NH and SH) closest to the TC4 sample region are shown in Figure 4 for comparison. Figure 4 suggests that almost all of the air sampled during TC4 came from the tropical NH, with only 4% of air sampled having methane amounts less than 1750 ppbv, indicating no significant unmixed stratospheric or SH air was sampled, except during a short flight segment on August 6, the low methane "tail" in Figure 4. *Pfister et al.* [2010] estimate that only 10–30% of air sampled in the troposphere during TC4 comes from the NH midlatitudes poleward of 25 N during the mission, which is consistent with this tracer data. Further, the lack of any data in the upper left quadrant of Figure 4 with $CH_4 < 1750$ ppbv and O3 > 70 ppbv indicates no significant stratospheric influence to the upper troposphere occurred during TC4.

[29] Comprehensive reactive nitrogen measurements (NO, NO_2, HNO_3, PAN, PNA) were made from the NASA DC-8 during TC4, and we consider them here. During TC4, *Scheuer et al.* [2010] found that HNO_3 was depleted on ice crystals in cirrus, and that it was enhanced in a thin layer just below cirrus by sedimenting and sublimating particles. In clouds, HNO_3 is strongly anti-correlated with CWC, because it is soluble (plot not shown). In midlatitudes near convection, *Bertram et al.* [2007] have reported a compelling relationship between the NO_x/HNO_3 ratio in an air parcel and the time since convection lifted the air from the lower into the upper troposphere. We tried to use the reactive nitrogen data from TC4 to do a similar "convective clock" analysis. Because of the frequency of convection and the non-conservation of HNO_3 in cirrus during TC4, the air parcel "age' since convection cannot be determined using this method. It is likely that this method works much better in mid-latitudes than in the tropics because the frequency of convection is much less.

[30] Further examination of the NO_2/NO_x ratio using NO_2 data from OMI and lightning data by *Bucsela et al.* [2010] suggests that lightning NO_x enhancement can be between 1.5 and 2.5 times the NO_x background, but there is also less lightning NO_x in tropical marine convection than in mid-latitude continental thunderstorms that are associated with midlatitude fronts. The upper tropospheric relationship of NO_x with O_3 is uncorrelated, indicating that the production of new ozone from lightning NO_x might happen downstream, but is not a dominant process within TC4 maritime convection. While the ratio of total reactive nitrogen (NO_y) to ozone has been used to indicate ozone production potential [*Ridley et al.*, 2006], in the actively convective TC4 "racetrack" region NO_y and O_3 are also uncorrelated (like NO_x and HNO_3, plot not shown), and is not useful for data interpretation here. PAN observations in the TTL (J. Elkins, personal communication, 2009, plot not shown) suggest that a significant amount of PAN (greater than 30 ppt) is vertically transported out of the boundary layer into the upper troposphere. PAN is not water-soluble and does not deposit on ice particles, so that reactive nitrogen can be transported vertically into the TTL and horizontally in the upper troposphere.

3.2. Case Studies of Convective Transport

3.2.1. July 24, 2007, the "Thor" Flight

[31] On the morning of July 24, 2007, the DC-8 and the ER-2 were to sample a developing thunderstorm complex in the ITCZ system at about 5 deg N, 85 deg W. The DC-8 was to extensively sample the boundary layer in the actively developing storm, and then to ascend through the storm and to sample cirrus in the outflow region to characterize convective transport and mixing. Although the flight was a success, it was cut short by a lightning strike to the DC-8. This was the only flight during the TC4 mission that sampled the core of such an actively developing storm.

[32] A Geostationary Operational Satellite (GOES) enhanced infrared satellite image overlain with the ER-2 and DC-8 flight tracks is shown in Figure 5a. The prevailing wind in the cirrus anvils of the convective cells is NE at 40 kt, and one can see this in the cloud pattern, as the anvils stream off to the SW. One can also see the more orderly "race track" pattern flown by the ER-2 above the cirrus, as opposed to the flight pattern taken by the DC-8 after it was hit by lightning. The cloud physics lidar (CPL), making measurements from the ER-2, provides context for the DC-8 in situ measurements taken inside the convective cell. Figure 5b shows a three-dimensional CPL image of the cirrus anvil, and the coincident DC-8 flight track, colored by in situ ozone concentration. Ozone was 16 ppbv in the boundary

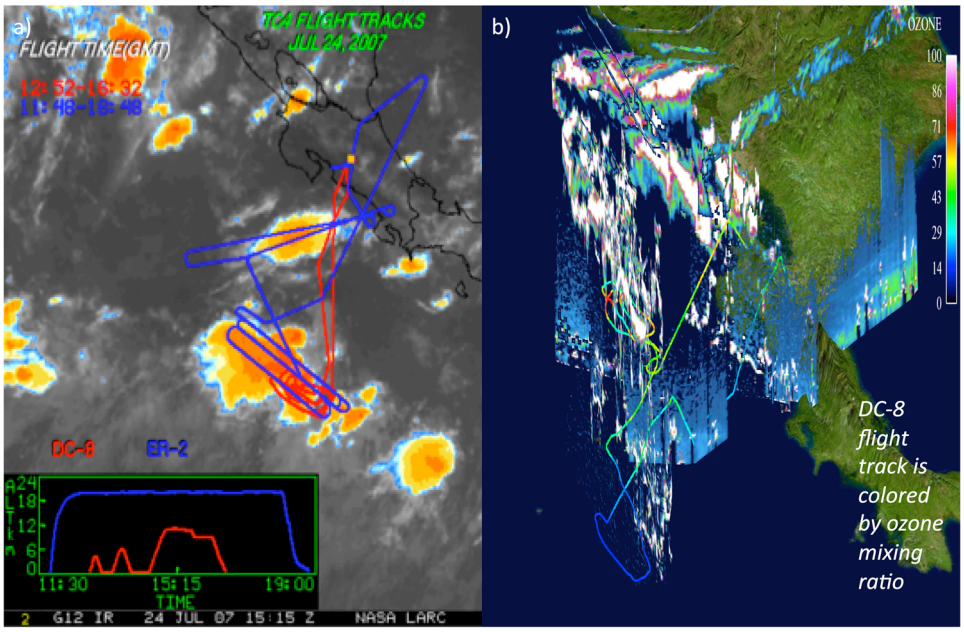

Figure 5. A composite of images from July 24, 2007, when the DC-8 flew underneath the ER-2 through a developing convective system and was hit by lightning. (a) A GOES visible image showing clouds during the high-altitude portion of the DC-8 flight through active convection. The DC-8 (blue) and ER-2 (red) flight tracks are superimposed on this image, which was provided by Patrick Minnis, NASA Langley. (b) A 3-dimensional view of the CPL lidar image of cloud tops and the DC-8 track (colored by ozone) through the storm. The image shows low ozone in the boundary layer (16 ppbv), moderate ozone in the lower troposphere, and large variability in ozone sampled in the racetrack loops 3–4 km below the cloud tops.

layer (BL) beneath the storm, typical of low BL ozone measured during TC4, increasing to 30–35 ppb at 3–4 km, as expected. The CPL shows that the cirrus cloud tops extend to 14–15 km, so the DC-8 in-cloud sampling occurred at about 3–4 km below the tropopause. One can see that the cirrus are ragged and uneven, and that the ozone inside them is highly variable, between 30 and 75 ppbv.

[33] The DC-8 sampled inside the developing cloud anvils at 11 km, 225 hPa, and penetrated the core of the storm where the ambient temperature was −47°C, so the cloud particle phase was ice. The 2DS cloud probe measured very large spikes in the condensed water content during this segment of the flight, when the DC-8 passed through strong convective turrets, shown in Figure 6. Figure 6 also shows the large vertical velocity of 20 m/s that was measured by MMS.

[34] A simple calculation of ozone production is possible in this very fresh convection. Using TC^4 measured ozone production rates of 1.1–3.2 ppbv/hour (Morris et al., submitted manuscript, 2010), with 2 m/s as a typical mean vertical velocity occurring over a vertical transport distance of 10 km, only 0.75–4.4 ppbv of ozone can be made during vertical transport. This is much smaller than the 14–19 ppbv difference between the low O_3 mixing ratios of 30–35 ppbv measured in the convective cloud and BL O_3 of 16 ppbv. The higher O_3 mixing ratios measured in the turrets also indicate that this air was not transported from the boundary layer without significant mixing to 10–11 km (225 hPa), where our sampling occurred. O_3 generation by electrical corona discharge may be possible [*Minschwaner et al.*, 2008]. This process is still somewhat speculative, and Minschwaner et al. estimate a total generation of 2×10^{28} molecules of O_3 in the highly electrified storm they studied, which is not enough to account for the O_3 difference between TC^4 BL and convective cores.

[35] Figure 7 shows a time series of tracers measured while the DC-8 sampled the convection at 10–11km. This corresponds to the upper two "loops" shown in Figure 5b, which also shows the large inhomogeneity of the convective cloud.

[36] There is a striking anti-correlation between CWC and ozone, with high ozone values (65–70 ppb) measured where CWC is low ("no cloud"), and lower ozone values (30–35 ppbv) measured inside the clouds. Positive vertical winds (figure not shown) are also anti-correlated with ozone. This strong anti-correlation between ozone and clouds persists throughout the TC4 data set.

[37] There is a positive correlation during this flight between carbon monoxide and ozone, indicating some aged pollution in the upper tropospheric background air, and vertical advection of relatively clean lower tropospheric air. However, this result is not consistent during upper tropospheric sampling on other flights. Correlations between ozone and horizontal wind direction, and between ozone and oxides of nitrogen are not significant during this flight (not shown), nor are they significant during the "racetrack" sampling in the upper troposphere for the mission as a whole. This indicates that convection dominates in redistributing ozone, and in this region it is more significant as a process for creating ozone variability than horizontal advection and in situ photochemistry.

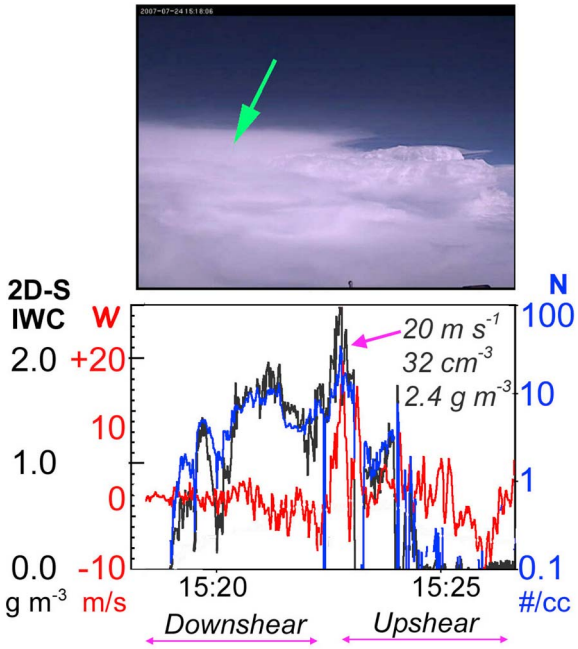

Figure 6. (top) A photograph from the DC-8 forward-looking video that shows convective turrets in the vigorous convection sampled on July 24, 2007. (bottom) Data from 11 km in the location of the green arrow in the video still. The vertical velocity was measured in situ by the MMS on the DC-8, in red, and ice water content (black) and particle density (blue) were measured by the 2D-S cloud probe. The peak vertical velocity of 20 m/s occurs with the large ice water concentration of 2.4 g/m3, indicated on the plot.

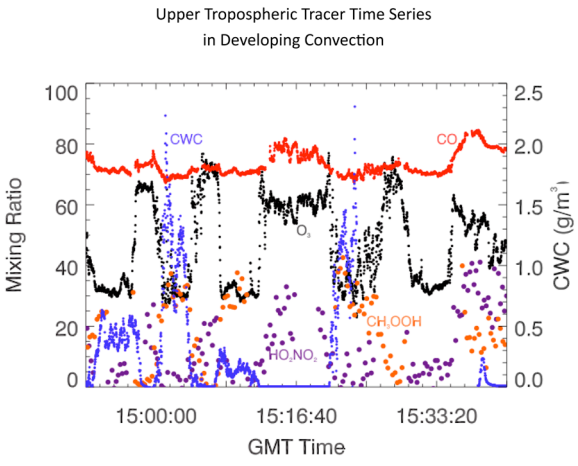

Figure 7. Time series of condensed cloud water content (blue), ozone (black), carbon monoxide (red), methyl-hydrogen peroxide, CH_3OOH (orange) and peroxy-nitric acid, HO_2NO_2 (purple) during racetrack portion of the 24 July flight in actively developing convection. The scale for the condensed cloud water content measured by the CVI and 2DS instruments is on the right-hand side, in g/m^3. Ozone, CWC and CH_3OOH are anti-correlated, while CO and HO_2NO_2 are positively correlated with O_3.

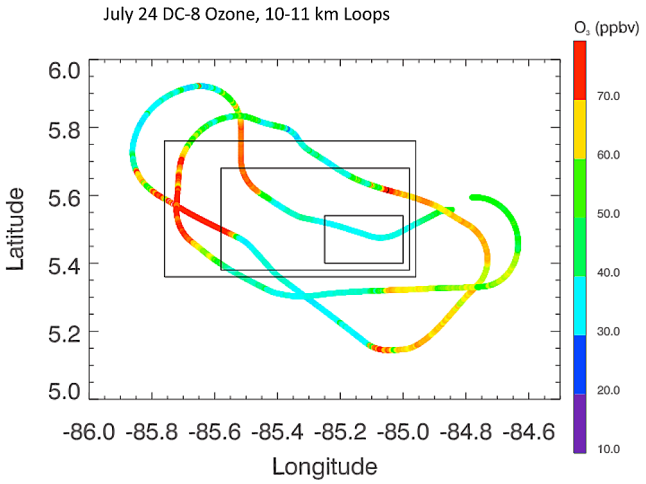

Figure 8. Map (degrees latitude and longitude) of the racetrack portion of the flight, colored by ozone using the same scale as shown in the 3-D image in Figure 5b. The black boxes show approximate nadir footprints of OMI (smallest), SCIAMACHY (medium), and GOME2 (largest).

[38] While relatively low ozone concentrations in the upper troposphere can be an effective indication of convective influence, this argument needs to be complemented by examining concentrations of a "positive" tracer for convection. Methyl hydrogen peroxide (CH_3OOH, MHP) is a convenient convective tracer to use in this case, because it is enhanced in the lowermost atmosphere but it is not significantly soluble. *Cohan et al.* [1999] have shown that MHP in very fresh convection can be elevated up to 6 times over the upper tropospheric background, but decays in the upper troposphere with a chemical lifetime of 1–2 days.

[39] Figure 7 shows CO, O_3, MHP and pernitric acid, (NO_2HO_2, PNA) measured during two of the 11 km (225 hPa) sampling loops, along with averages obtained just prior to the ascent during the boundary layer run. The addition of the tracers shows that three distinct air types were sampled. Air that has recently been transported into the upper troposphere with low O_3 has high MHP and low PNA. This freshly convected air can be seen at 14:05 and 15:10 GMT, corresponding to the DC-8 passage through convective turrets shown in Figure 6. The second air type, background tropospheric air with high O_3 mixing ratios (>60 ppb) has relatively high PNA and low MHP, with examples centered near 14:59 and 15:07 GMT on the plot. There are also slightly higher values of CO and CH_4 (not shown) that are anti-correlated with O_3, with examples at around 15:17 and 15:38 GMT on the plot.

[40] Figure 8 shows the flight track from above, indicating the location of these different air types, which stay coherent between flight loops. The ozone color scale in this plot is the same as shown in the 3-D image in Figure 5b. The variability has spatial scales of the order of 10–50 km. Figure 8 also shows approximate footprint sizes of various ultraviolet and visible satellite backscatter instruments. The smallest is that of OMI, with a nadir pixel of approximately 12 km × 24 km. The spatial scales of the different observed air types are similar to the OMI nadir footprint, so it is feasible that OMI

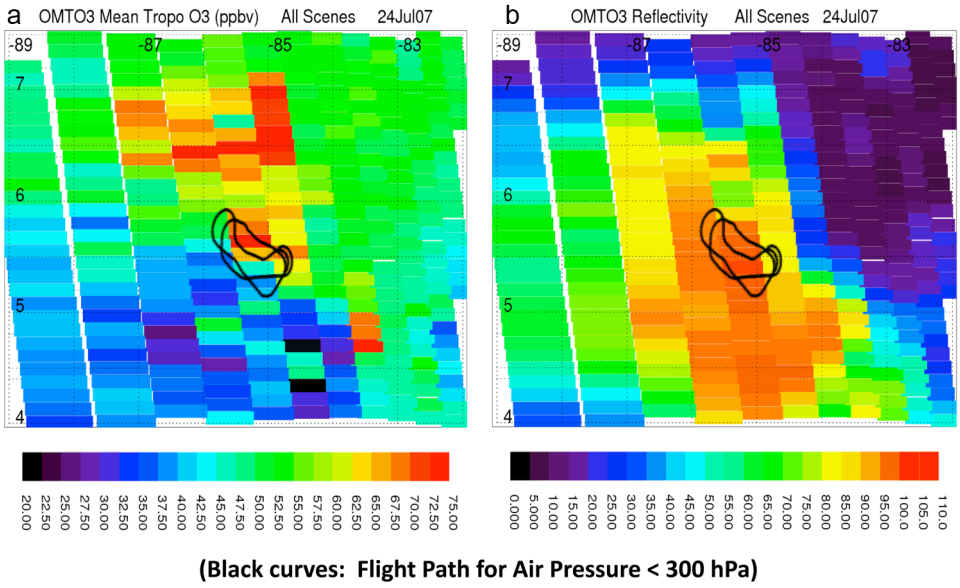

Figure 9. (a) OMI/MLS tropospheric ozone mean volume mixing ratio (units ppbv) measured during the 18:30 Z overpass of the AURA satellite on July 24, 2007. The OMI swath is 2600 km wide. (b) The corresponding OMI reflectivity measurements. The DC-8 flight path for this day is shown in both Figures 9a and 9b. These OMI measurements correspond to the detailed aircraft tracer measurements taken from the DC-8 was circling near 225 hPa inside the active convective system that are shown in Figures 7 and 8. A loop of GOES satellite images (not shown) clearly shows the convective outflow streaming off to the SW, coincident with the lower O_3 values measured by OMI.

data can resolve ozone variability that is caused by convective processes, and the data have been used previously to retrieve ozone mixing ratios inside deep convective clouds [*Ziemke et al.*, 2009].

[41] The mean tropospheric ozone volume mixing ratios (ppbv) calculated between the tropopause and 300–450 hPa derived using OMI and Microwave Limb Sounder (MLS) data are shown in Figure 9a for the AURA overpass occurring closest to this flight (18:30 Z on July 24, 2007). This overpass occurred about 4 h after the DC-8 sampled inside the developing convection as described above. Examination of GOES images using loops provided by the Langley TC4 satellite group (P. Minnis et al., Cloud properties determined from GOES and MODIS data during TC4, submitted to *Journal of Geophysical Research*, 2010) shows that during this time the convective system continued to grow, with outflow streaming off to the southwest. Figure 9b shows the reflectivity measured by OMI during the AURA overpass, and shows the location of the cloud anvil. The DC8 flight path while the plane was circling near the tops of the convective clouds is shown on both Figures 9a and 9b. In this area there is a large contrast in mean ozone mixing ratios from <40 ppbv (blues) to >65 ppbv (reds).

[42] These derived OMI column-mean mixing ratios appear to be consistent with the in situ measurements taken several hours earlier in the developing storm, showing variability due to the contrast between ozone mixing ratios in freshly lofted and background upper tropospheric air. The OMI data suggest a region of relatively polluted air adjacent to the cloud, with ozone mixing ratios similar to measurements with elevated CO from the DC-8 (Figure 7). Lower ozone seen by OMI in the SW corner of the scene corresponds to the convective outflow region of the cloud, as verified by GOES image loops and the prevailing NE wind. As expected, OMI/MLS data do not capture the finer-scale ozone variability shown in the in situ measurements. However, the larger perspective that OMI offers shows the extent of lowered ozone in the convective outflow to the southwest of the system. A histogram of the OMI mean tropospheric ozone measurements for the entire region peaks at 49 ppbv (+/−10 ppbv), which is consistent with the in situ ozone distribution shown in Figure 2a, and is indicated in the clear regions of Figure 9a. Further, in the "racetrack" region the maximum and minimum ozone mixing ratios of ~70 ppbv and ~35 ppbv retrieved using the OMI data are similar to those measured in situ from the DC-8 (Figure 7). Since sonde and lidar ozone data are not available in deep convective clouds, this comparison of in situ and OMI ozone measurements provides a unique validation of the OMI/MLS mixing ratios derived inside convection.

3.2.2. August 5, 2007, Convective Outflow

[43] On this day DC-8, ER-2 and WB-57 flew a well-coordinated pattern in convective outflow, first identified in satellite images. In section 2 we presented a movie showing the relationship between the DC-8 flight track and the cirrus outflow from the convection sampled, including mages of the cirrus from both the CALIOP instrument on CALIPSO and the CPL. Figure 10 focuses on measurements from the DC-8. Figure 10a shows a 3-dimensional picture of the CPL cirrus image and in situ ozone data (bottom) and the in situ carbon monoxide data (top). During this flight the boundary layer and lower troposphere are quite polluted compared

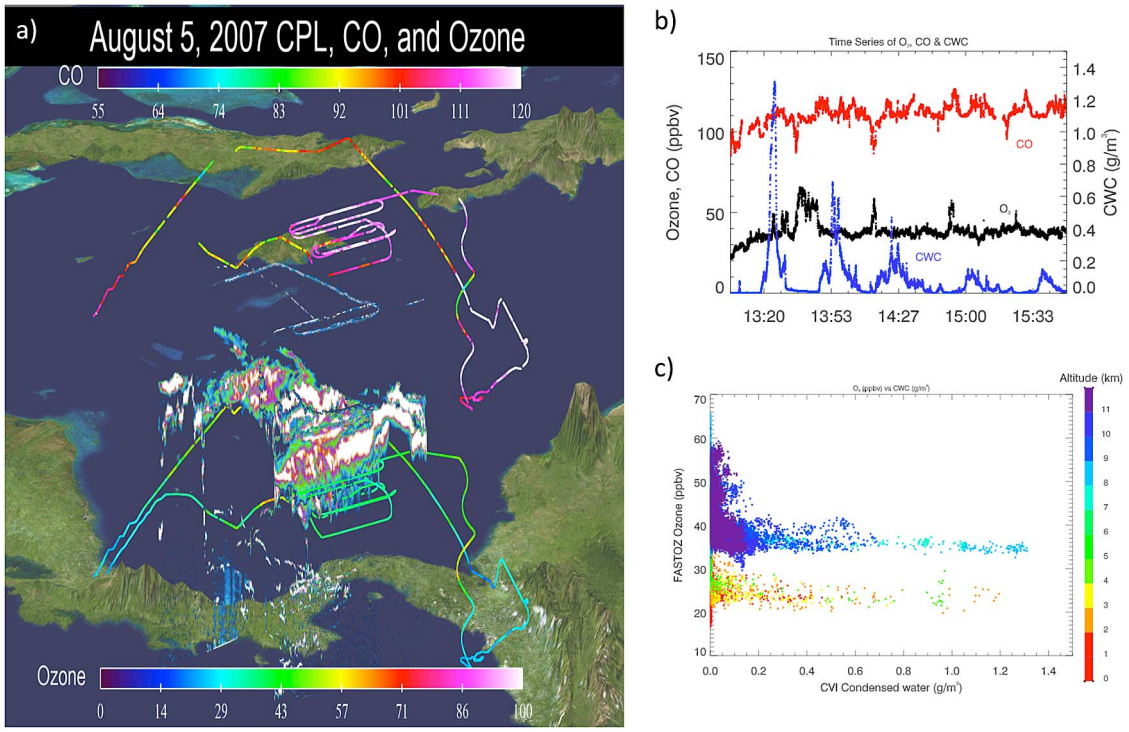

Figure 10. Several plots of ozone, CO, condensed cloud water and cloud images are shown here from the August 5th flights of the DC-8 and ER-2. These images correspond to the movie showing the 3-dimensional CALIOP, CPL and DC-8 cloud data all together. (a) A 3-dimensional still image of the entire DC-8 and ER-2 flights. The CPL shows the location of the cirrus anvils sampled, with cloud tops at 14 km, 3–5 km above the DC-8. The DC-8 flight track is colored by in situ ozone. Overlain above this image is a repeated DC-8 flight track, colored by carbon monoxide. (b) The time series of CO (red) ozone (black) and CWC (blue) from the DC-8 during the racetracks. The trace shows spikes of high ozone and lower CO on the dry side of the racetrack, outside of the cirrus anvil. (c) A correlation plot of ozone and condensed cloud water, colored by altitude.

with the July 24th flight shown above, and on this day, O_3 and CO are almost always anti-correlated, as opposed to their positive correlation on July 24.

[44] The 3-dimensional picture in Figure 10a shows that the highest DC-8 racetrack pattern was flown inside the cirrus, 3–4 km below the anvil tops at 14–15 km. Figure 10b shows the O_3, CO and CWC traces from the racetrack sampling. The spikes of higher ozone (60 ppbv) coincide with lower CO (90 ppbv) on the side of the racetrack where the DC-8 turns around outside of the cloud, as indicated by the absence of CWC. This trace is shown because it is a good example of vertical advection of polluted air out of the boundary layer, and of the in cloud/out of cloud difference in air composition. Figure 10c is a plot of O_3 (y axis) versus CWC (x axis) from the whole flight, colored by altitude. It is interesting to note the predominance of O_3 concentrations of ~ 25 ppbv in the lower clouds, and O_3 ~ 35–40 ppbv in the anvil clouds. This again suggests that convection does not transport undiluted air directly into the upper troposphere.

3.3. Regional Statistics

[45] In this section we look at the combined data set from all of the local upper troposphere (8–12 km) sampled during TC4. Figure 11 shows the O_3:CWC relationship in all the data colored by altitude, similar to Figure 10c. The cloudy

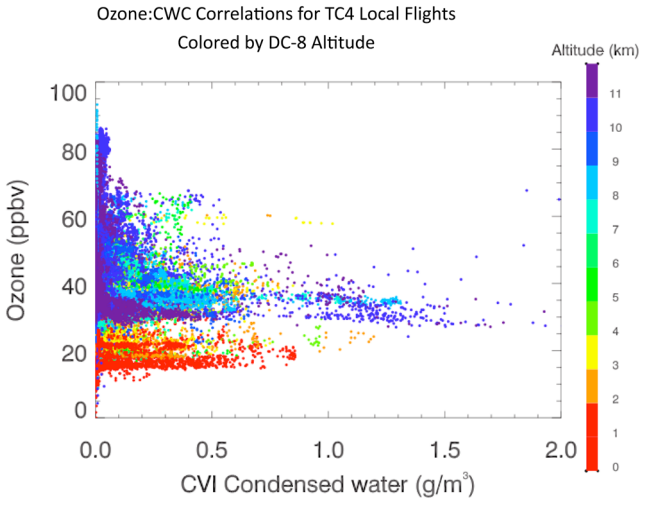

Figure 11. A composite correlation plot of ozone and condensed cloud water content measured by the CVI instrument in the upper troposphere during all of the "racetrack" flights. The data points are colored by altitude.

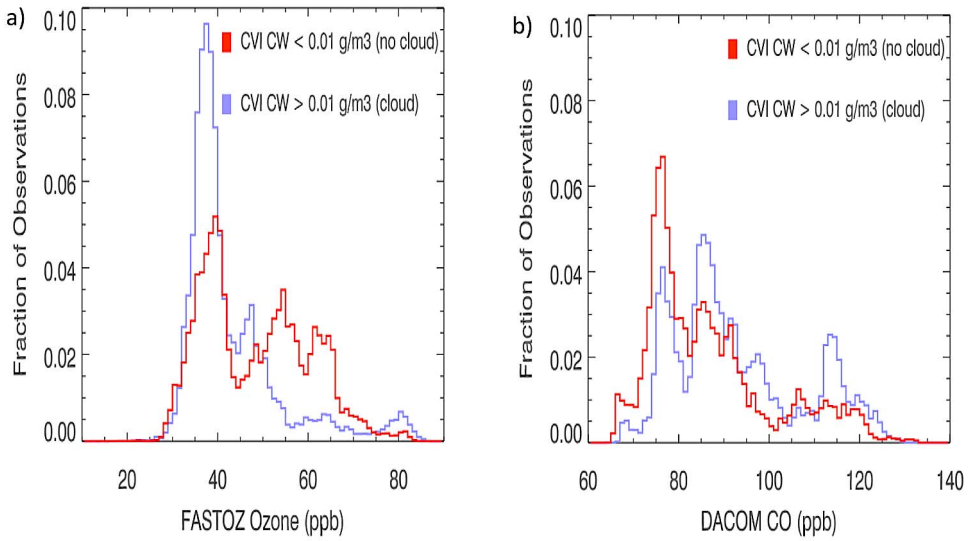

Figure 12. (a) Normalized probability distribution histograms for ozone data measured during upper tropospheric "racetracks" when the DC-8 was in a cloud (blue) and not in a cloud (red). A threshold of 0.01 g/m^3 of equivalent liquid condensed cloud water was chosen to divide the data set. The choice of this threshold is described in the text. (b) Normalized probability distributions for carbon monoxide inside (blue) and outside (red) of clouds, similar to Figure 12a for ozone.

areas clearly have less ozone than the clear ones, with all of the high ozone occurring where CWC approaches zero. A somewhat arbitrary value of 0.01 g/m^3 was chosen to divide the data set into "cloudy" and "not cloudy" bins for looking at ozone probability distributions. The CVI out-of-cloud baseline is lower than this (~0.002 g/m^3), but a higher value is chosen to avoid including a CVI cloud exit hysteresis signal as a cloud. The ozone distribution is not very sensitive to this choice, tested between 0.002 – 0.02 g/m^3.

[46] Figures 12a and 12b show "in cloud" and "out of cloud" probability histograms of ozone and carbon monoxide. The peak of the in-cloud probability distribution occurs at 37 ppbv, which is representative of in-cloud O_3 mixing ratios measured in both active convection and convective outflow as shown above. There are relatively few measurements of O_3 between 50 and 75 ppbv in the cloudy data. The small peak in O_3 at 80 ppbv in cloud did not reach the upper troposphere by vertical transport directly from the lower troposphere, because there were no measurements of ozone greater than 75 ppbv below 10 km. The DC-8 must have flown through a small, cloudy pollution plume, but there are so few data points that this small plume does not affect our conclusions significantly.

[47] In contrast, the "out of cloud" ozone measurements in the upper troposphere show ozone concentrations between 50 and 75 ppbv in about 50% of the air sampled. The CO histograms show a peak in "clean" air with CO of 75 ppbv outside of the clouds, perhaps representing a tropical upper tropospheric background. There is a somewhat more even distribution of CO occurring in clouds, reflecting the large amount of variability in CO in the lower troposphere. The cloudy air contains more CO than the clear air, indicating that vertical convective transport is a net source of "dirty" air to the upper troposphere.

3.4. Comparison With Sondes and Tracer Profiles

[48] An analysis of vigorous tropical convection in the Western Pacific by *Solomon et al.* [2005] documents the transport of air containing very low ozone to the tropical TTL region, and also shows the usefulness of examining a profile of low ozone measurements for establishing the altitude of maximum convective outflow. From our analysis of in cloud and out of cloud probability distributions of ozone measured in the upper troposphere, we find a minimum in the histogram occurring at 44 ppbv, with a sharp peak in the cloudy mixing ratios below this value (Figure 12a). Using this number as a threshold for "low ozone," we calculate the fraction of measurements of low ozone in 500 m bins throughout the troposphere for the Panama and Alajuela sondes, as well as for the WB-57 and DC-8 local ozone profiles. This distribution is shown in Figure 13a. For comparison, Figure 13b shows this distribution with a threshold of 28 ppbv, the largest ozone mixing ratio measured during DC-8 boundary layer runs.

[49] There is a large difference between the sonde and the aircraft low ozone measurement distributions, which we attribute to a sampling difference. The sondes were mainly launched in background air, and the planes targeted convection, so the difference is between clear and cloudy air. The DC-8 distribution peaks just below 10 km, while the WB-57 peaks just above, and this is most likely because of the extensive DC-8 in cloud sampling. Evident from Figures 13a and 13b is that convective outflow peaks at 10–11 km, a lower altitude in this region than in the Western Pacific. This is consistent with an average cloud top height of 14.2 km derived from the CPL data [*Chang et al.*, 2010], also lower than the Western Pacific. Figure 13b also indicates that only 5–10% of air sampled in the maximum outflow region comes directly from the boundary layer without mixing.

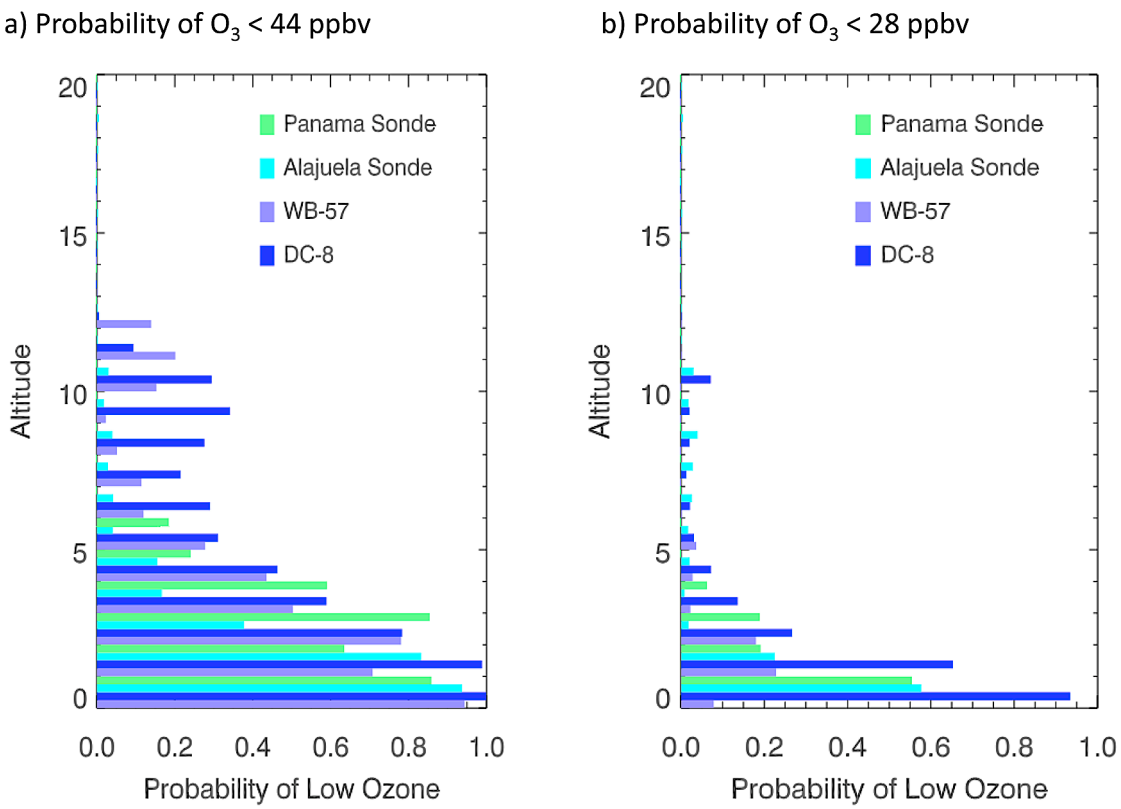

Figure 13. A profile of the probability of occurrence of low ozone in 500 m vertical bins for the WB-57 and the DC-8 TC4 ozone data from local flights, and for the Alajuela and Panama sonde measurements. (a) The probability of measuring O_3 < 44 ppbv, a threshold derived from the probability distribution shown in Figure 12 to include the "in cloud" low ozone peak. (b) For comparison, P(O_3 < 28 ppbv), which includes all measured boundary layer values, but less than 25% of ozone measured at 2 km and above.

[50] Given the difference between sonde and aircraft measurements of maximum convective outflow, we looked more carefully at the distribution of MHP. The altitude profile of MHP for all TC4 local flights is shown in Figure 14, with the upper tropospheric maximum occurring at 10–11 km, substantiating the aircraft measurements of low ozone. For comparison to fresh convective measurements, the inset (Figure 14b) is a correlation plot of O_3 and MHP measured during the July 24 case study. With the exception of 4–5 data points, all of the elevated MHP (>300 pptv) occurs at ozone mixing ratios of less than 40 ppbv. During this flight the distributions of MHP in the boundary layer ($O_3 \leq 20$ ppbv), above the boundary layer in the lower troposphere (2–3 km, $O_3 \sim 30$ ppbv), and in the upper tropospheric cloudy measurements are similar. The highest uncertainty of the MHP measurements occurs in humid air, i.e., the marine boundary layer.

[51] We also tested the profile of another low altitude tracer measured from the DC-8 and WB-57, in this case the total of measurements of organic bromine species that are produced by marine life in the ocean surface waters. Figure 15a shows a composite of total organic bromine measurements. It is evident from the organic bromine enhancement in the upper troposphere that the altitude of maximum convective outflow occurs at 10–11 km. For comparison,

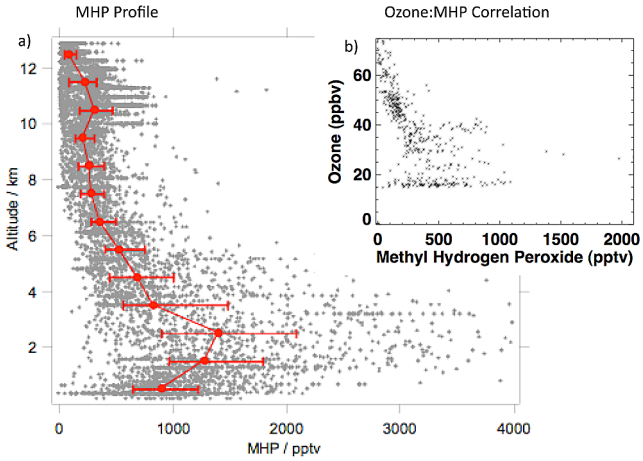

Figure 14. (a) Altitude profile of MHP mixing ratio as measured from DC8 in all local flights during TC4. Gray crosses are individual (1 s) points. Red trace is the median of 1-km altitude bins; whiskers show the first and third quartiles for these bins. (b) For comparison, a correlation plot of O_3 and MHP from the July 24 flight in very fresh, developing convection.

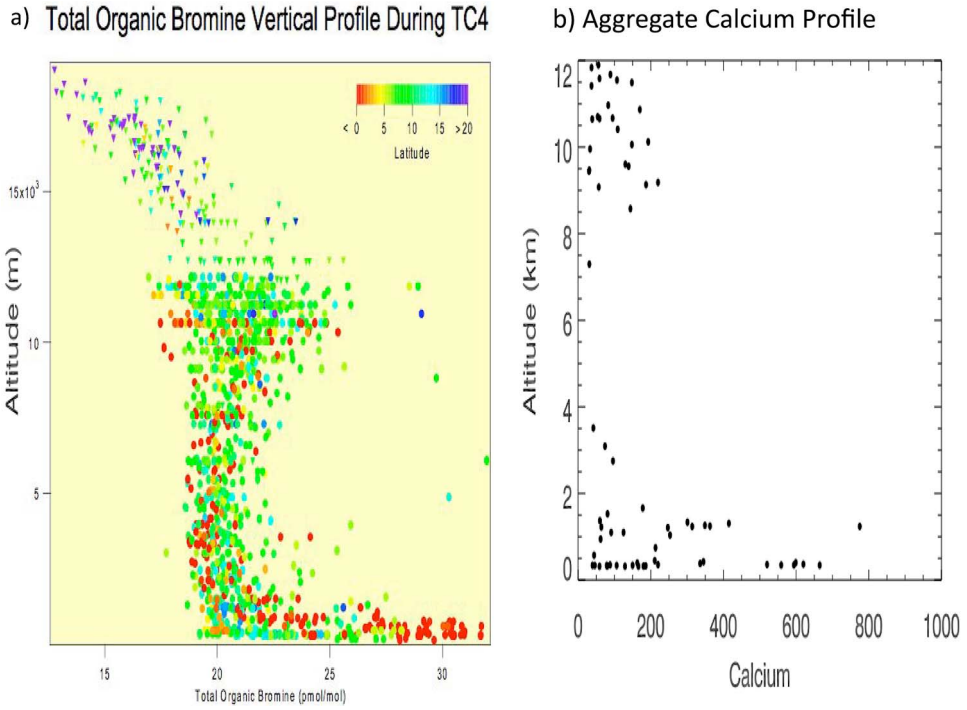

Figure 15. (a) The profile of total organic bromine measured by gas chromatography performed on whole air samples taken from the NASA ER-2 and the DC-8 during the TC4 field campaign. Total organic bromine is shown here as a tracer for boundary later air. (b) An aggregate profile of calcium ion concentrations taken from all available bulk air samples taken during the TC4 local flights. Calcium is used as a proxy for Saharan dust.

Figure 15b shows the profile of calcium ions measured in bulk aerosol samples as a proxy for dust. In regions impacted by Saharan dust, dust is enhanced in nearby cirrus (K. Froyd, personal communication, 2010). Since the Saharan dust layer is typically found at 2–3 km, this would suggest a significant contribution to convective outflow from this altitude, consistent with what we find most likely using ozone. Very simple mass balance calculations using ozone, bromine and calcium measurements at 10–11 km suggest that about 50% of the mass in this region of the upper troposphere has been transported upwards from the lower troposphere.

[52] All ozone measured in the upper troposphere above 6 km is > 30 ppbv, with medians > 40 ppbv, and all boundary layer ozone measurements during TC^4 are < 27 ppbv with a 20 ppbv median. Either boundary layer air is mixing perfectly with mid-tropospheric air (O3 ~ 45 ppbv) during the rapid ascent to 10–11 km, or more likely the convection is lofting a significant amount of air from above the BL, which has also been observed to happen in continental thunderstorms [*Pickering et al.*, 1988]. This is supported by the temperature and dewpoint soundings from sondes launched from the DC-8 into the convective clouds during racetrack flights. Skew-T plots from these soundings show that while there is always a wind shear defining the top of the boundary layer, often the temperature inversion is negligible and air is at or very near saturation up to 500–600 hPa (3–5.5 km), where there is frequently another small temperature inversion. Further examination of MMS vertical velocities in convection show well-defined peaks in positive vertical velocities (>2 m/s) occurring at pressures of 820, 680, 460 and 225 hPa in the developing 07/24 convection, and at 800 and 600 hPa in the more mature convective cell sampled on 08/05. Mass conservation implies that compensating convergence or entrainment is also occurring at these altitudes.

4. Summary

[53] The ITCZ is a region of complex diabatic processes and small-scale mixing, and typically general circulation models do not perform well in this environment. Extensive sampling of the convectively active upper tropospheric ITCZ during TC^4 by multiple aircraft provides a unique opportunity to use observations to understand convective transport processes. We found the troposphere to be well-mixed tropical background air with well-aged pollution, no distinct plumes of stratospheric air and very few plumes of freshly polluted air. Due to the frequency of convection and cloud processing of air, reactive nitrogen ratios are not effective in this region for studying convective processes. Further, since both clean and dirty BL air is lofted in this region, use of CO as a convective tracer is problematic. By examining aircraft data from two flight days during which the ER-2 and the DC-8 sampled an actively developing convective system, and a more mature system generating convective outflow, we find that the most robust relationship is an anti-correlation between ozone and the amount of condensed water in a convective cloud.

[54] When we extend this analysis to a combined data set from DC-8 sampling of the upper troposphere in the "racetracks" pattern, we find that the peak of the ozone

measurement distribution in cloud is 37 ppbv. Carbon monoxide measurements imply that there is a net transfer of polluted air from the lower to the upper troposphere. Boundary layer ozone measurements are tightly distributed around 20–22 ppbv, lower than the value found in convective clouds by roughly 15 ppbv. Measurements of vertical velocity in active convection and Lagrangian measurements of the ozone production rate from a sonde in convection imply that although the ozone production rate can be large, it is probably not capable of adding the missing 15 ppbv of ozone during transport. Measurements of methyl hydrogen peroxide do not help to discriminate between transport of air from above the boundary layer into the upper troposphere, and boundary layer air that has mixed significantly (50%) during the rapid (~15–20 min) vertical transport to 10–11 km. We note that the sensitivity of MHP measurements in humid air, and therefore the lower troposphere, is relatively poor. However, vertical velocity profiles, temperature and dewpoint soundings, and the lack of ozone < 28 ppbv in convective outflow suggest that entrainment of air and rapid vertical transport from above the boundary layer is more likely.

[55] The altitude of maximum convective outflow measured during TC4 is found to be between 10 and 11 km, characterized by the maximum probability of measuring low ozone, and maximums in the vertical distributions of MHP and total organic bromine. This is significantly lower than predicted by the theoretical model of *Folkins et al.* [2006a], which calculates the maximum amount of flux divergence to occur at 12 km, but is consistent with cloud top heights that are also lower (14.2 km [*Chang et al.*, 2010]), so that in both cases the altitude of maximum convective outflow occurs about 4 km below the cloud tops. Similarly, it is also lower than indicated by measurements from sondes in the Western Pacific [*Solomon et al.*, 2005]. A rough mass balance calculation of the amount of convective transport using mean ozone, bromine and calcium ions ("dust") suggests that 50% of the air in the upper troposphere below the TTL in this region has been vertically transported there by convection. There does not appear to be a significant amount of undiluted boundary layer air being vertically transported to the upper troposphere, even in very active convection.

[56] **Acknowledgments.** The authors thank the NASA Middle Atmosphere and Tropospheric Chemistry Programs for funding, and Program Managers Michael Kurylo and Hal Maring for launching sondes from the DC-8. We thank Lenny Pfister for all sorts of meteorological information and consultation. We thank Gary Morris for providing the Las Tablas sonde data, and we thank Alex Bryan and David Lutz for launching all of these Panama sondes. Holger Voemel provided the Alajuela ozonesonde data, and Ru-shan Gao provided ozone measurements from the WB-57. Ross Salawitch and Tim Canty provided the plot of total organic bromine, and we are grateful for many helpful discussions. We also thank Mario Rana for DC-8 fast-response tracer lag correlations and Ali Aknan for "Chemical Digital Atlas" plots and calculations of statistical vertical tracer distributions during various tropospheric aircraft field missions (http://www-air.larc.nasa.gov/cgi-bin/datlas). We are grateful to K.A. Masserie and E. Dlugokencky at NOAA CMDL for the Barbados and Bahia methane measurements, and to Pat Minnis and his group for the GOES satellite images and loops.

References

Avery, M., D. Westberg, H. Fuelberg, R. Newell, B. Anderson, S. Vay, G. Sachse, and D. Blake (2001), Chemical transport across the ITCZ in the central Pacific during an El Niño-Southern Oscillation cold phase event in March–April 1999, *J. Geophys. Res.*, *106*(D23), 32,539–32,553, doi:10.1029/2001JD000728.

Bertram, T., et al. (2007), Direct measurements of the convective recycling of the upper troposphere, *Science*, *315*, 816–820, doi:10.1126/science.1134548.

Bucsela, E., et al. (2010), Lightning-generated NO_x seen by the Ozone Monitoring Instrument during NASA's Tropical Composition, Cloud and Climate Coupling Experiment (TC4), *J. Geophys. Res.*, *115*, D00J10 doi:10.1029/2009JD013118.

Chang, F.-L., P. Minnis, J. K. Ayers, M. J. McGill, R. Palikonda, D. A. Spangenberg, W. L. Smith, and C. R. Yost (2010), Evaluation of satellite-based upper troposphere cloud top height retrievals in multilayer cloud conditions during TC4, *J. Geophys. Res.*, *115*, D00J05, doi:10.1029/2009JD013305.

Cohan, D., M. Schultz, D. Jacob, B. Heikes, and D. Blake (1999), Convective injection and photochemical decay of peroxides in the tropical upper troposphere: Methyl iodide as a tracer of marine convection, *J. Geophys. Res.*, *104*(D5), 5717–5724, doi:10.1029/98JD-1963.

Dibb, J., et al. (2003), Aerosol chemical composition in Asian continental outflow during TRACE-P: Comparison to PEMWest B, *J. Geophys. Res.*, *108*(D21), 8815, doi:10.1029/2002JD003111.

Fairlie, T. D., M. A. Avery, R. B. Pierce, J. Al-Saadi, J. Dibb, and G. Sachse (2007), Impact of multiscale dynamical processes and mixing on the chemical composition of the upper troposphere and lower stratosphere during the Intercontinental Chemical Transport Experiment: North America, *J. Geophys. Res.*, *112*, D16S90, doi:10.1029/2006JD007923.

Folkins, I., M. Lowenstein, J. Podolske, S. J. Oltmans, and M. Profitt (1999), A barrier to vertical mixing at 14 km in the tropics: Evidence from ozonesondes and aircraft measurements, *J. Geophys. Res.*, *104*(D18), 22,095–22,102, doi:10.1029/1999JD900404.

Folkins, I., C. Braun, A. M. Thompson, and J. C. Witte (2002), Tropical ozone as an indicator of deep convective outflow, *J. Geophys. Res.*, *107*(D13), 4184, doi:10.1029/2001JD001178.

Folkins, I., P. Bernath, C. Boone, L. J. Donner, A. Eldering, G. Lesins, R. V. Martin, B.-M. Sinnhuber, and K. Walker (2006a), Testing convective parameterizations with tropical measurements of HNO_3, CO, H_2O, and O_3: Implications for the water vapor budget, *J. Geophys. Res.*, *111*, D23304, doi:10.1029/2006JD007325.

Folkins, I., P. Bernath, C. Boone, K. Walker, A. M. Thompson, and J. C. Witte (2006b), The seasonal cycles of O_3, CO and convective outflow at the tropical tropopause, *Geophys. Res. Lett.*, *33*, L16802, doi:10.1029/2006GL026602.

Froidevaux, L., et al. (2008), Validation of Aura Microwave Limb Sounder stratospheric ozone measurements, *J. Geophys. Res.*, *113*, D15S20, doi:10.1029/2007JD008771.

Gregory, G. L., E. V. Browell, and L. S. Warren (1988), Boundary layer ozone: An airborne survey above the Amazon Basin, *J. Geophys. Res.*, *93*(D2), 1452–1468, doi:10.1029/JD093iD02p01452.

Joiner, J., and A. P. Vasilkov (2006), First results from the OMI rotational Raman scattering cloud pressure algorithm, *IEEE Trans. Geosci. Remote Sens.*, *44*, 1272–1282.

Joiner, J., et al. (2009), Accurate satellite-derived estimates of the tropospheric ozone impact on the global radiation budget, *Atmos. Chem. Phys.*, *9*(13), 4447–4465, doi:10.5194/acp-9-4447-2009.

Lawson, R. P., D. O'Connor, P. Zmarzly, K. Weaver, B. A. Baker, Q. Mo, and H. Jonsson (2006), The 2D-S (stereo) probe: Design and preliminary tests of a new airborne, high speed, high-resolution particle imaging probe, *J. Atmos. Oceanic Technol.*, *23*(11), 1462–1477, doi:10.1175/JTECH1927.1.

Lawson, R. P., E. J. Jenson, B. Baker, and Q. Mo (2010), Microphysical and radiative properties of tropical clouds investigated in TC4 and NAMMA, *J. Geophys. Res.*, *115*, D00J08, doi:10.1029/2009JD013017.

Levelt, P. F., et al. (2006), The Ozone Monitoring Instrument, *IEEE Trans. Geosci. Remote Sens.*, *44*, 1093–1101, doi:10.1109/TGRS.2006.872333.

McGill, M. J., D. L. Hlavka, W. D. Hart, J. D. Spinhirne, V. S. Scott, and B. Schmid (2002), The Cloud Physics Lidar: Instrument description and initial measurement results, *Appl. Opt.*, *41*, 3725–3734.

McPeters, R., M. Kroon, G. Labow, E. Brinksma, D. Balis, I. Petropavlovskikh, J. P. Veefkind, P. K. Bhartia, and P. F. Levelt (2008), Validation of the AURA Ozone Monitoring Instrument total column ozone product, *J. Geophys. Res.*, *113*, D15S14, doi:10.1029/2007JD008802.

Minschwaner, K., L. E. Kalnajs, M. K. Dubey, L. M. Avallone, P. C. Sawaengphokai, H. E. Edens, and W. P. Winn (2008), Observation of enhanced ozone in an electrically active storm over Socorro, NM: Implications for ozone production from corona discharges, *J. Geophys. Res.*, *113*, D17208, doi:10.1029/2007JD009500.

Pearson, R.W., and D.H. Stedman (1980), Instrumentation for fast response ozone measurements from aircraft, in *Atmospheric Technology*, vol. 12, pp. 51-55, Natl. Cent. for Atmos. Res., Boulder, Colo.

Pfister, L., H. B. Selkrk, D. O. Starr, P. A. Newman, and K. H. Rosenlof (2010), A meteorological overview of the TC4 mission, *J. Geophys. Res.*, *115*, D00J12, doi:10.1029/2009JD013316.

Pickering, K. E., R. R. Dickerson, G. J. Huffman, J. F. Boatman, and A. Schanot (1988), Trace gas transport in the vicinity of frontal convective clouds, *J. Geophys. Res.*, *93*(D1), 759–773, doi:10.1029/JD093iD01p00759.

Pickering, K. E., et al. (1996), Convective transport of biomass burning emissions over Brazil during TRACE-A, *J. Geophys. Res.*, *101*(D19), 23,993-24,012, doi:10.1029/96JD00346.

Ridley, B. A., M. A. Avery, J. V. Plant, S. A. Vay, D. D. Montzka, A. J. Weinheimer, D. J. Knapp, J. E. Dye, and E. C. Richard (2006), Sampling of chemical constituents in electrically active convective systems: Results and cautions, *J. Atmos. Chem.*, *54*, 1-20, doi:10.1007/s10874-005-9007-5.

Sachse, G., G. Hill, L. Wade, and M. Perry (1987), Fast-response, high-precision carbon monoxide sensor using a tunable diode laser absorption technique, *J. Geophys. Res.*, *92*(D2), 2071–2081, doi:10.1029/JD092iD02p02071.

Scheuer, E., J. E. Dibb, C. Twohy, D. C. Rogers, A. J. Heymsfield, and A. Bansomer (2010), Evidence of nitric acid uptake in warm cirrus clouds during the NASA TC4 campaign, *J. Geophys. Res.*, *115*, D00J03, doi:10.1029/2009JD012716.

Schoeberl, M. R., et al. (2007), A trajectory-based estimate of the tropospheric ozone column using the residual method, *J. Geophys. Res.*, *112*, D24S49, doi:10.1029/2007JD008773.

Scott, S. G., T. P. Bui, K. R. Chan, and S. W. Bowen (1990), The meteorological measurement system on the NASA ER-2 aircraft, *J. Atmos. Oceanic Technol.7*(4)525540doi:10.1175/1520-0426(1990)007<0525:TMMSOT>2.0.CO;2.

Solomon, S., D. W. J. Thompson, R. W. Portmann, S. J. Oltmans, and A. M. Thompson (2005), On the distribution and variability of ozone in the tropical upper troposphere: Implications for tropical deep convection and chemical-dynamical coupling, *Geophys. Res. Lett.*, *32*, L23813, doi:10.1029/2005GL024323.

Spencer, K. M., et al. (2009), Inferring ozone production in an urban atmosphere using measurements of peroxynitric acid, *Atmos. Chem. Phys.*, *9*(11), 3697–3707, doi:10.5194/acp-9-3697-2009.

Thompson, A. M., et al. (2010), Convective and wave signatures in ozone profiles over the equatorial Americas: Views from TC4 (2007) and SHADOZ, *J. Geophys. Res.*, doi:10.1029/2009JD012909, in press.

Toon, O. B., et al. (2010), Planning and overview of the Tropical Composition, Cloud and Climate Coupling Experiment, *J. Geophys. Res.*, 115, D00J04, doi:10.1029/2009JD013073.

Twohy, C. H., A. J. Schanot, and W. A. Cooper (1997), Measurement of condensed water content in liquid and ice clouds using an airborne counterflow virtual impactor, *J. Atmos. Oceanic Technol.*, *14*(1), 197–202, doi:10.1175/1520-0426(1997)014<0197:MOCWCI>2.0.CO;2.

Vasilkov, A. P., J. Joiner, R. Spurr, P. K. Bhartia, P. F. Levelt, and G. Stephens (2008), Evaluation of the OMI cloud pressures derived from rotational-Raman scattering by comparisons with satellite data and radiative transfer simulations, *J. Geophys. Res.*, *113*, D15S19, doi:10.1029/2007JD008689.

Winker, D. M., W. H. Hunt, and M. J. McGill (2007), Initial performance assessment of CALIOP, *Geophys. Res. Lett.*, *34*, L19803, doi:10.1029/2007GL030135.

Ziemke, J. R., S. Chandra, and P. K. Bhartia (2001), "Cloud slicing": A new technique to derive upper tropospheric ozone from satellite measurements, *J. Geophys. Res.*, *106*(D9), 9853–9867, doi:10.1029/2000JD900768.

Ziemke, J. R., J. Joiner, S. Chandra, P. K. Bhartia, A. Vasilkov, D. P. Haffner, K. Yang, M. R. Schoeberl, L. Froidevaux, and P. F. Levelt (2009), Ozone mixing ratios inside tropical deep convective clouds from OMI satellite measurements, *Atmos. Chem. Phys.*, *9*(2), 573–583, doi:10.5194/acp-9-573-2009.

E. Atlas, Division of Marine and Atmospheric Chemistry, Rosenstiel School of Marine and Atmospheric Sciences, University of Miami, 4600 Rickenbacker Causeway, Miami, FL 33149, USA.

M. Avery and C. Trepte, Atmospheric Composition Branch, Science Directorate, NASA Langley Research Center, MS 475, Hampton, VA 23681, USA. (melody.a.avery@nasa.gov)

D. Blake, School of Physical Sciences, University of California, 570 Rowland Hall, Irvine, CA 92697, USA.

P. Bui, Atmospheric Science Branch, Earth Science Division, NASA Ames Research Center, MS 245-5, Moffett Field, CA 94035-1000, USA.

J. Crounse, D. McCabe, and P. Wennberg, Chemistry Department, California Institute of Technology, 100 North Mudd Laboratory, MC 150-21, Pasadena, CA 91125, USA.

J. Dibb and E. Scheuer, Institute for the Study of Earth, Oceans, and Space, University of New Hampshire, 39 College Rd., Durham, NH 03824-3525, USA.

G. Diskin, Chemistry and Dynamics Branch, NASA Langley Research Center, MS 483, Hampton, VA 23681, USA.

J. Joiner, Atmospheric Chemistry and Dynamics Branch, Code 613.3, NASA Goddard Space Flight Center, Greenbelt, MD 20771, USA.

P. Lawson, SPEC Inc., 3022 Sterling Cir., Ste. 200, Boulder, CO 80301, USA.

M. McGill, Mesoscale Atmospheric Processes Branch, Code 613.1, NASA Goddard Space Flight Center, Greenbelt, MD 20771, USA.

D. Rogers and C. Twohy, Department of Oceanic and Atmospheric Science, Oregon State University, 244 Strand Ag Hall, Corvallis, OR 997331, USA.

G. Sachse, National Institute of Aerospace, 100 Exploration Way, Hampton, VA 23666, USA.

K. Severance, Systems Engineering Directorate, NASA Langley Research Center, MS 458, Hampton, VA 23681, USA.

A. Thompson, Department of Meteorology, Pennsylvania State University, 510 Walker Bldg., University Park, PA 16802, USA.

J. Ziemke, Goddard Earth Sciences and Technology Center, University of Maryland Baltimore County, 5523 Research Park Dr., Ste. 320, Baltimore, MD 21228, USA.